Magnetic loss versus frequency in non-oriented steel sheets and its prediction: minor loops, PWM, and the limits of the analytical approach

Magnetic loss versus frequency in non-oriented steel sheets and its prediction: minor loops, PWM, and the limits of the analytical approach.

Carlo Ragusa[1,a], Hanyu Zhao (赵浛宇)[1,2], Olivier de la Barrière[3], Mahmood Khan[1], Carlo Appino[4], and Fausto Fiorillo[4]
[1]Energy Department, Politecnico di Torino, Torino 10129, Italy
[2]Province-Ministry Joint Key Laboratory of Electromagnetic Field and Electrical Apparatus, Hebei University of Technology, 300130 Tianjin, China
[3]Laboratoire SATIE, CNRS - ENS Cachan, F-94230 Cachan, France
[4]Nanoscience and Materials Division, INRIM, Torino, Italy

The Pulse Width Modulation (PWM) technique is commonly used to supply modern high-speed electrical machines. The fundamental frequency is typically in the kilohertz range, with switching frequencies of several tens of kilohertz, as determined by the new SiC or GaAs based power transistors modules. Switching introduces minor loops in the major hysteresis cycle, with durations of the order of 100 µs or lower, with the resulting magnetization dynamics influenced by strong skin effect. However, since these minor loops have relatively small amplitude, their constitutive equation may be described by an equivalent permeability (real or complex), depending on the mean slope of the minor loop and its static energy loss. By retrieving this permeability, the classical loss is straightforwardly calculated by analytical solution of the Maxwell's equations. In this work, we measure and calculate, according to the quasi-linear approximation for the minor loops, the magnetic energy losses of 0.194 mm thick non-oriented Fe-Si 3.2% sheets subjected to PWM induction waveform. Minor loop peak amplitudes ranging between 50 mT and 0.2 T and frequencies up to 10 kHz are investigated. The results are consistent with the proposed model, to within 5%.

***Index Terms*—Magnetic losses, Pulse Width Modulation, Loss separation, Skin effect.**

I. Introduction

Pulse width Modulation (PWM) is widely applied to supply modern electrical machines because of the advantages offered by power electronics for driving the machines at their maximum efficiency on a wide speed range [1][2]. In addition, it can improve the electromagnetic compatibility requirements of the actuator [3]. Fig. 1 shows an example of a PWM waveform and the associated major and minor hysteresis cycles, for a frequency modulation index $m_f = 5$. Because of the presence of nested minor loops, the PWM supply is the source of extra magnetic losses, which should conveniently be evaluated [4]. Loss modeling under such non-conventional supply conditions has been investigated in the past, assuming negligible skin effect [5]. In present devices, however, increasing supply frequencies are used and fundamental frequencies in the kilohertz range can be found [6], together with switching frequencies of several tens of kilohertz, favored by use of the new SiC or GaAs based power transistors modules [7][8]. Under such conditions, the dynamics of the minor loops is strongly influenced by the skin effect, which brings about substantial interpretative difficulties in the theoretical modeling of the losses. In a previous paper [9], the classical loss related to cycles of small amplitude at high frequencies was computed in Fe-Si sheets by assuming a linear magnetic constitutive equation for the material. In this way, the skin effect could easily be accounted for through a linear diffusion model. The loss separation showed then that the well-known linear behavior of the excess loss vs. the square root of frequency, predicted by the Statistical Theory of Losses (STL) [10], could be retrieved up to about 10 kHz. On the other hand, an increase of the hysteresis loss component at high frequencies can be predicted, because of the non-uniform induction profile across the sheet thickness imposed by the skin effect. However, this might negligibly affect the loss decomposition, because the hysteresis loss could be largely overcome by the classical and excess loss components at such frequencies.

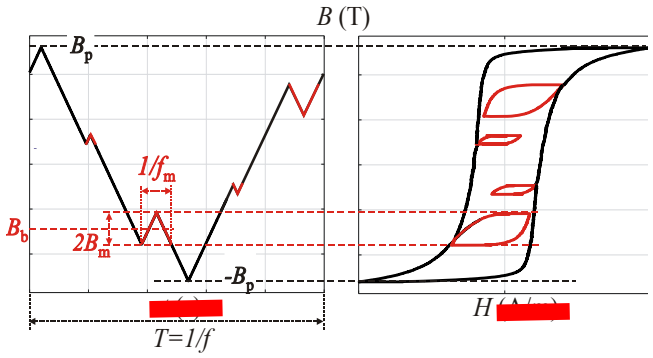

Fig. 1 - Example of PWM waveform and associated hysteresis cycles for a frequency modulation index of $m_f = 5$. The major loop is in black, the nested minor loops are in red.

In this paper we calculate the dynamic losses at low induction values taking into account the skin effect by use of a properly identified complex permeability in the analytical derivation of the classical loss. In addition, the frequency dependent hysteresis loss component is computed taking into account the actual induction profile and the excess loss is predicted by the STL up to the highest frequencies. The model is applied to the experiments obtained in a 0.194 mm thick Fe-Si 3.2% sheet, expressly developed for high frequency applications. Induction values, ranging from 50 mT to 0.2 T, have been considered, both for symmetric hysteresis loops and minor loops associated with PWM waveforms. The calculations show good agreement with the measured losses,

[a] Corresponding author, e-mail: carlo.ragusa@polito.it

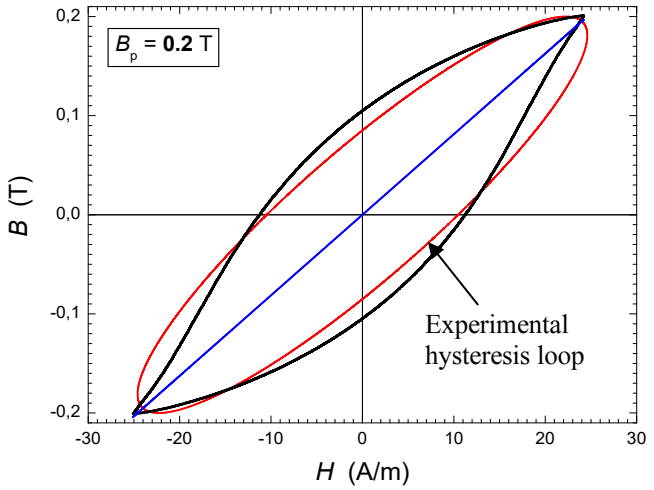

Fig. 2 - Experimental quasi-static loop at peak induction $B_p = 0.2$ T in the NO Fe-Si sheet. It is approximated either by a straight $B(H)$ line ($\mu = 8.13\cdot10^{-3}$ Tm/A) or by the elliptic loop of identical area associated with the complex permeability $\underline{\mu} = \mu' - j\mu''$, with $\mu' = 7.35\cdot10^{-3}$ Tm/A and $\mu'' = 3.47\cdot10^{-3}$ Tm/A.

with maximum uncertainty of the order of 5%.

II. Modeling the Minor Loops at High Frequencies

The classical loss in magnetic sheets under negligible skin effect and sinusoidal flux density of peak value B_p is predicted by the standard formula

$$W_{class}\left(B_p, f\right) = (\pi^2/6)\cdot\sigma d^2 B_p^2 f\,, \qquad (1)$$

where d is the thickness of the sheet, σ is the conductivity, and f is the frequency [10]. However, at sufficiently high frequencies the eddy current counterfield will impose an increasingly non-uniform induction profile across the sheet thickness and the assumption of uniform induction is no more satisfied. In this case, modeling of the magnetic loops becomes a difficult task, because it involves the solution of Maxwell equations taking into account a strongly non-linear magnetic constitutive equation. To this end, numerical methods are generally applied, which do not lead to simple expressions for the energy loss. With minor loops of relatively small amplitude, such as to comply, for instance, with the Rayleigh law, we might reasonably attempt to adopt a permeability-based magnetic constitutive equation of the material [9]. Such permeability would then be introduced in the electromagnetic diffusion equation, in order to achieve induction profile and classical energy loss. Hysteresis loops at very low frequencies (a few hertz) have therefore been carried out as a function of peak induction B_p. Two types of permeability have therefore been considered:

- The permeability μ taken as the ratio between the peak induction B_p and the peak field H_p.
- The complex permeability $\underline{\mu} = \mu' - j\mu''$, which takes into account the phase shift appearing under quasi static conditions between the sinusoidal B and the first harmonic of H, giving rise to the hysteresis loss. Its modulus is still equal to the ratio B_p/H_p. The imaginary part is identified in such a way that the hysteresis loss W_{hyst} of the measured loop and that of the equivalent elliptical cycle coincide, according to the equation $\mu'' = W_{hyst}/(\pi\cdot H_p^2)$. An example of quasi-static measured and equivalent elliptical loops at $B_p = 0.2$ T in the investigated NO Fe-Si sheet is shown in Fig. 2.

A. Classical loss component

With the minor static loop represented as a first approximation by the modulus of the permeability $\mu = B_p/H_p$, the classical loss is straightforwardly obtained by solving the Maxwell's diffusion equation

$$W_{cl}(f) = \frac{\pi}{2}\cdot\frac{\lambda B_p^2}{\mu}\cdot\frac{\sinh\lambda - \sin\lambda}{\cosh\lambda - \cos\lambda} \qquad [\mathrm{J/m^3}], \qquad (2)$$

where $\lambda = \sqrt{\pi\sigma\mu d^2 f}$. By adopting the complex permeability $\underline{\mu} = \mu' - j\mu''$ as magnetic constitutive equation, we get [11]

$$W_{class}(B_p, f) = \frac{\pi}{2}\frac{B_p^2}{|\underline{\mu}|}\cdot\frac{\left(\lambda' - \lambda''\right)\sinh\left(\lambda' - \lambda''\right) - \left(\lambda' + \lambda''\right)\sin\left(\lambda' + \lambda''\right)}{\cosh\left(\lambda' - \lambda''\right) - \cos\left(\lambda' + \lambda''\right)}, \qquad (3)$$

where λ' and λ'' are related to the permeability according to

$$\lambda = \lambda' + j\lambda'' = \sqrt{\frac{\omega\sigma|\underline{\mu}|d^2}{2}}\cdot\left(\sqrt{\frac{1+\mu'/|\underline{\mu}|}{2}} - j\cdot\sqrt{\frac{1-\mu'/|\underline{\mu}|}{2}}\right) \qquad (4)$$

B. Estimated hysteresis and excess losses.

In order to account for the dependence on frequency of the hysteresis loss caused by the frequency evolution of the induction profile, we shall take advantage of the local character of the associated dissipation mechanism (elementary Barkhausen jumps and extremely localized eddy currents). We consider then first that the hysteresis loss depends on the peak induction according to a power law $W_{hyst} = K\cdot B_p^{\alpha}$. The parameters K and α are identified by best fitting of the hysteresis loss measured at $B_p = 50$ mT, 0.1 T, and 0.2 T. For our 0.194 mm thick Fe-Si sheet, we obtain $K = 159.7$ and $\alpha = 1.8$ (with W_{hyst} expressed in J/m^3). Having calculated the induction profile $b_p(x)$, where x is the distance from sheet midplane, as a solution of the diffusion equation using the adopted model permeability, W_{hyst} is immediately obtained for the sheet of thickness d

$$W_{hyst}\left(B_p, f\right) = \frac{1}{d}\int_{-d/2}^{d/2} K\cdot b_p^{\alpha}(x)\,\mathrm{d}x \qquad (5)$$

Regarding the excess loss, it is assumed dependent on the measured peak induction B_p, the averaged value of $b_p(x)$ [5], and is calculated as

$$W_{exc}\left(B_p, f\right) = 8.76\cdot\sqrt{\sigma G S V_0\left(B_p\right)}B_p^{1.5}\sqrt{f}\,, \qquad (6)$$

where the dimensionless constant $G = 0.1356$, S is the cross-sectional area of the sheet sample, and the statistical parameter V_0 is an increasing function of B_p [5]. $V_0(B_p)$ is identified by means of standard loss measurements under sinusoidal flux at frequencies where the skin effect can be ignored [10] (in the present case up to about 2 kHz).

C. Experimental results

The magnetic energy loss $W(f)$ has been measured in 0.194 mm thick Fe-(3.2 wt%)Si sheets. Ring samples of

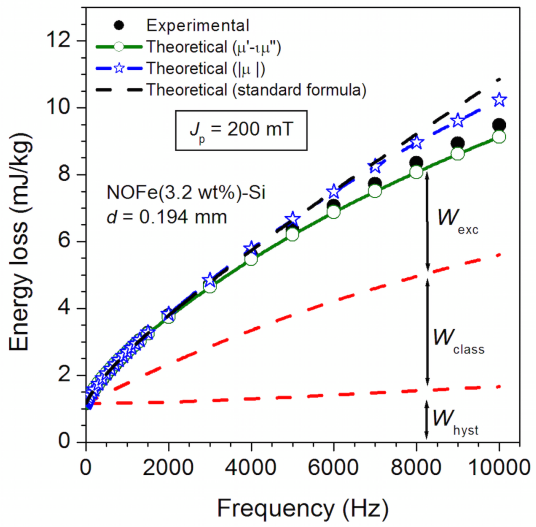

Fig. 3 - Energy loss $W(f)$ measured in a 0.194 mm thick Fe-(3.2 wt%)Si sheet up to 10 kHz at peak polarization J_p = 200 mT. The J_p value is low enough to fulfill the Rayleigh law and the skin effect fully develops above a few kHz. The measured $W(f)$ is predicted best by adopting the quasi-static complex permeability at J_p = 200 mT as the material constitutive equation. To note the increase of the hysteresis loss component W_{hyst} with the frequency.

outside diameter 100 mm and inside diameter 80 mm, annealed 2 hours at 760 °C after punching, have been tested at B_p values ranging between 50 mT and 0.2 T up to 10 kHz. The measurements have been performed by means of a broadband calibrated hysteresisgraph-wattmeter with digital control of the induction waveform. Three interpretative models have been applied to the obtained results.

1) A standard model neglecting skin effect and using (1) for the calculation of the classical loss.

2) A linear diffusion model using the quasi-static modulus of permeability $\mu = B_p/H_p$.

3) A linear diffusion model assuming the complex quasi-static permeability $\underline{\mu} = \mu' - j\mu''$ as the material constitutive equation.

Fig. 3 provides an example of experimental $W(f)$ behavior obtained up to 10 kHz for B_p = 0.2 T compared with the loss predictions based on the previous three approaches. It shows how the complex permeability model (3) leads to the best agreement with the measured $W(f)$. The hysteresis $W_{hyst}(f)$ and excess $W_{exc}(f)$ loss components calculated according to (5) and (6) are also provided. It is noted the slight increase of $W_{hyst}(f)$ at the highest frequencies. Similar fitting results are obtained for B_p = 50 mT and B_p = 0.1 T.

III. The PWM regime

Two-level PWM induction waveforms have been measured in the same 0.194 mm thick Fe-(3.2 wt%)Si ring sample. An example of the obtained induction waveform and hysteresis loops is shown in Fig. 1. The waveforms are characterized by the modulation index $m_f = F/f$, the ratio of the switching frequency F to the fundamental frequency f, and B_p. To estimate the energy loss, we decompose the whole PWM induction loop into the major loop (in black in Fig. 1), and the nested minor loops (in red color). The period of the major loop is T_M and the equivalent frequency is $f_M = 1/T_M$. The period of each minor loop is T_m and its equivalent frequency is $f_m = 1/T_m$. All the parameters of the PWM waveform are summarized in Table I. We model the related energy loss by calculating the hysteresis, classical and excess components, each of them resulting from the separate contributions of the major and the minor loops.

TABLE I: Parameters of the PWM induction regime

Symbol	Description
B_p	Peak value of the PWM induction waveform (or the major loop), assumed to be centered
$2{\cdot}B_m$	Peak to peak value of a given minor loop
B_b	Mean value of the induction on a given minor loop (bias)
f	Frequency of the PWM waveform
F	Switching frequency of the PWM
m_f	Modulation index of the PWM, defined as $m_f = F/f$.
f_M	Equivalent frequency of the major loop, obtained as the inverse of the time spent on the major loop
f_m	Equivalent frequency on a given minor loop, obtained as the inverse of the duration of the minor loop

1) Loss associated with the major loop

The major loop is equivalent to a symmetric cycle of peak value B_p and frequency f_M, obtained under triangular induction waveform. For this case, the skin effect can be neglected [12] and the loss calculation is easily performed, as discussed in [5].

2) Loss associated with the minor loops

Each minor loop, characterized by the bias induction B_b, the peak-to-peak amplitude $2{\cdot}B_m$, and the equivalent magnetizing frequency f_m, is separately considered. Since f_m can be of several tens of kilohertz, the skin effect cannot be ignored. In addition, the minor loops are not centered, and their shape changes with the bias B_b. To simplify the matter, the following assumptions are made: a) the minor loops are swept with sinusoidal flux, with the parameters (B_b, B_m, f_m). This approximation makes it possible to use the complex permeability formalism defined above in solving the diffusion equation. b) The minor loops are assumed to be congruent in B, that is, a minor loop with parameters (B_b, B_m, f_m) starting from the anhysteretic curve, is congruent with the minor loop endowed with the same parameters hanging from the major cycle. We identify then the static complex permeability $\underline{\mu}(B_m, B_b)$ on the anhysteretic curve as a function of B_m and B_b. This procedure is described in Fig. 4. Here, the bias polarization is applied by a third winding, wound on the toroid and supplied by a stable DC current. Five values of B_b, up to 1.4 T, and $\pm B_m$ values ranging between 50 mT and 0.2 T have been selected. The different loss contributions from the minor loops at the typical PWM working frequencies have then been calculated as follows.

Classical *loss component.* The classical loss formula (3) is implemented, with the complex permeability pertaining to the specific (B_m, B_b) minor loop.

Hysteresis loss component. The integral (5) is calculated, with the coefficients K and ◘ duly considered as a function of B_m and B_b.

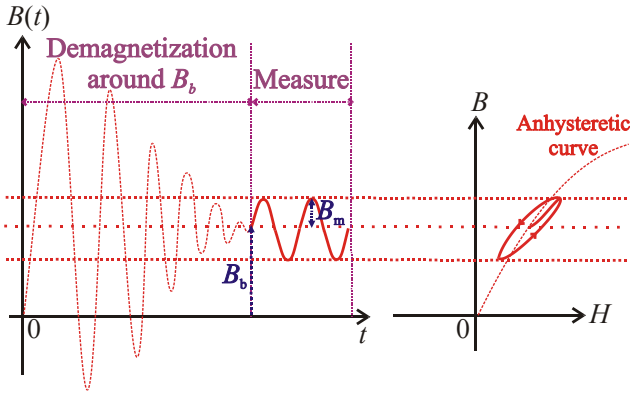

Fig. 4 – Acquisition method of the static complex permeability $\underline{\mu}(B_m, B_b)$ on the anhysteretic curve as a function of peak and bias induction pair (B_m, B_b). The bias value is generated by a third winding supplied by a stable constant current.

Excess loss component: Equation (6) is applied, now with V_0 depending on both B_m and B_b. A direct determination of $V_0(B_m, B_b)$ would require measurements and loss separation at each bias induction B_b, a cumbersome procedure. We have therefore resorted to an approach, discussed in [13], where V_o is calculated as a function of the induction bias. The following formula holds

$$V_0(B_m, B_p) = \frac{1}{k} < \sqrt{1/\mu} >^2 \quad , \tag{7}$$

where k is a suitable constant introduced in [13], μ is the differential permeability, and the brackets indicate averaging over the given minor cycle. For small amplitude B_m, we can write

$$V_o\left(B_m, B_b\right) \approx V_o\left(B_m, B_b = 0\right) \frac{\left|\underline{\mu}\left(B_m, B_b = 0\right)\right|}{\left|\underline{\mu}\left(B_m, B_b\right)\right|}, \tag{8}$$

and we can therefore proceed to implement the loss separation procedure for symmetric minor loops.

Fig. 5 provides an example of PWM loss measurement at 1 kHz in the 0.194 mm thick non-oriented Fe-Si sheet. The major loop is described between ± 1.3 T and the modulation index m_f is varied between 5 and 13. The experimental dependence of the PWM energy loss is predicted to good extent by the model.

IV. Conclusion

It is shown that a simplified approach to the constitutive equation of a magnetic sheet at low induction values, expressed in terms of complex permeability, in combination with the Statistical Theory of Losses, makes it possible to account in analytical terms for the dependence of the energy loss of minor loops up to frequencies involving large skin effect. It is shown, in particular, that the case of the two-level PWM waveform with nested minor loops can be simply treated by the model, resulting in good agreement with the experimental results.

V. References

[1] E. Bostanci, Z. Neuschl, and R. Plikat, "Influence of phase magnetic couplings on phase current characteristics of multiphase BLDC machines with overlapping phase windings," *IEEE Trans. Magn.*, vol. 51, no. 9, pp. 1-13, 2015. doi: 10.1109/TMAG.2015.2430833

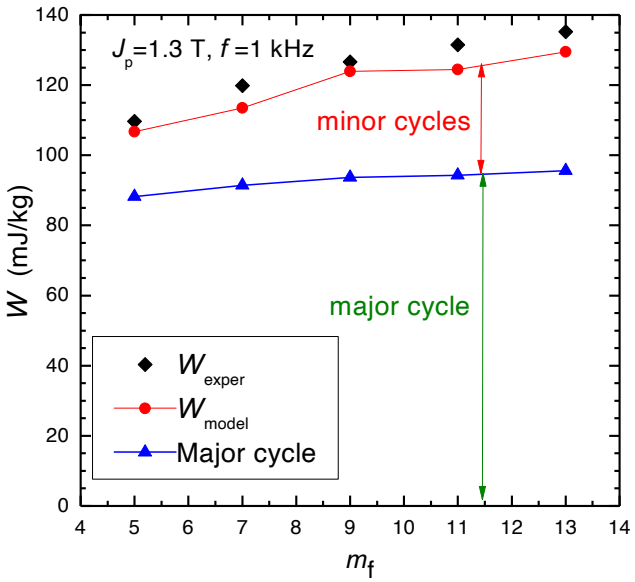

Fig. 5 – Non-oriented Fe-Si sheet of thickness 0.194 mm. Comparison of the energy losses measured at the peak polarization J_p = 1.3 T with PWM waveform as a function of the modulation index m_f at the fundamental frequency f = 1 kHz with the prediction of the model.

[2] M. Fakam, M. Hecquet, V. Lanfranchi, and A. Randria, "Design and magnetic noise reduction of the surface permanent magnet synchronous machine using complex air-gap permeance," *IEEE Trans. Magn.,* vol. 51, no. 4, pp. 1-9, 2015. doi: 10.1109/TMAG.2014.2360315

[3] M. Kamruzzaman, M. R. Barzegaran, and O. Mohammed, "EMI reduction of PMSM drive through matrix converter controlled with wide band gap switches," *IEEE Trans. Magn.* 2017. doi: 10.1109/TMAG.2017.2660443.

[4] Y. Takeda, Y. Takahashi, K. Fujiwara, A. Ahagon, and T. Matsuo, "Iron loss estimation method for rotating machines taking account of hysteretic property," *IEEE Trans. Magn.,* vol. 51, no. 3, pp. 1-4, 2015. doi: 10.1109/TMAG.2014.2357412.

[5] E. Barbisio, F. Fiorillo, and C. Ragusa, "Predicting loss in magnetic steels under arbitrary induction waveform and with minor hysteresis loops," *IEEE Trans. Magn.*, vol. 40, no. 4, pp. 1810-1819, 2004. doi: 10.1109/TMAG.2004.830510

[6] S. Jumayev et al., "The effect of PWM on rotor eddy-current losses in high-speed permanent magnet machines," *IEEE Trans. Magn.*, vol. 51, no. 11, pp. 1-4, 2015. doi: 10.1109/TMAG.2015.2438637

[7] X. Gong and J. A. Ferreira, "Comparison and reduction of conducted EMI in SiC JFET and Si IGBT-based motor drives," *IEEE Trans. Power Electron.*, vol. 29, no. 4, pp. 1757-1767, 2014. doi: 10.1109/TPEL.2013.2271301

[8] X. Yongxiang, Y. Qingbing, Z. Jibin, W. Baochao, and L. Junlong, "Periodic Carrier Frequency Modulation in Reducing Low-Frequency Electromagnetic Interference of Permanent Magnet Synchronous Motor Drive System," *IEEE Trans. Magn.*, vol. 51, no. 11, pp. 1-4, 2015. doi: 10.1109/TMAG.2015.2440293

[9] C. Ragusa H. Zhao, C. Appino, M. Khan, O. de la Barrière, and F. Fiorillo, "Loss decomposition in non-oriented steel sheets: the role of the classical losses," *IEEE Magn. Lett.*, vol. 7, pp. 1-5, 2016. doi: 10.1109/LMAG.2016.2604204

[10] G. Bertotti, "General properties of power losses in soft ferromagnetic materials," *IEEE Trans. Magn.*, vol. 24, no. 1, pp. 621-630, 1988.

[11] C. Beatrice, S. Dobák, E. Ferrara, F. Fiorillo, C. Ragusa, J. Füzer, and P. Kollár "Broadband magnetic losses of nanocrystalline ribbons and powder cores," *J. Magn. Magn. Mater.* vol. 420, pp. 317-323, 2016.

[12] C. Beatrice, C. Appino, O. de la Barrière, F. Fiorillo, and C. Ragusa, "Broadband magnetic losses in Fe-Si and Fe-Co laminations", *IEEE Trans. Magn.* vol. 50, pp. 6300504, 2014.

[13] O. de la Barrière, C. Ragusa, C. Appino, and F. Fiorillo, "Prediction of Energy Losses in Soft Magnetic Materials under Arbitrary Induction Waveforms and DC bias," *IEEE Trans. Ind. Electron.* vol. 64, pp. 2522-2529, 2017.